

SINDBAD: a Simulation Software Tool for Multi-energy X-Ray Imaging

Veronique REBUFFEL, Joachim TABARY, Mathieu TARTARE, Andrea BRAMBILLA,
Loick VERGER

CEA, LETI, MINATEC Campus, F-38054 Grenoble, France.

Phone: +33 438783103, Fax: +33 438785164; e-mail: veronique.rebuffel@cea.fr, joachim.tabary@cea.fr,
andrea.brambilla@cea.fr, mathieu.tartare@cea.fr, loick.verger@cea.fr

Abstract

The computer simulation of realistic radiographs has been proved to be an efficient tool for the design of X-ray systems, the specification of their components, the development of dedicated image processing methods and the final validation. Sindbad software has been developed at LDET laboratory for that purpose. The goal of this paper is to describe new developments of Sindbad allowing taking into account recently emerged semiconductor based X-ray detectors that offer new capabilities in counting mode with energy discrimination. A model of such detectors is proposed, considering both physical and electronics phenomena. The integration into Sindbad offers spectral imaging simulation functionalities in both radiography and tomographic mode. Examples highlight the energetic dependency of contrast. Validation has been performed, using for comparison semiconductor detectors developed in our laboratory. An example of quantification of beam-hardening artefact illustrates the influence of detector characteristics on image quality.

Keywords: simulation, radiography, detector modelling, multi-energy X-ray imaging.

1. Introduction

Computer simulations are a valuable tool to help the design stage of radiographic systems or to evaluate the efficiency of image processing techniques in radiography or tomography applications. For the simulated projection images being comparable to those obtained by a real X-ray system, the simulation tool should incorporate a good modelling of all the physics involved in the radiographic chain, a detailed description of the generator and the detector, and be able to handle efficiently complex phantoms.

The X-ray radiographic simulation software Sindbad [1], [2] has been developed at LDET laboratory for that purpose. It allows the modelling of any radiographic set-up, any object to be examined, and takes into account the various X-ray/matter interactions. Until now, Sindbad was proposing various detectors models (film, flat panel, scintillating screen coupled to CCD camera, photomultiplier), all working in integration mode, thus providing per pixel a single value, corresponding to the deposited energy integrated over the energy range.

Recently emerged semiconductor based X-ray detectors offer new capabilities in counting mode with energy discrimination [3], [4]. They give access to the energetic dependence of X-ray absorption. Energy sensitive detectors can potentially decrease image noise, enhance contrast, enable specific material imaging or material identification. Tomography artefacts are reduced. A lot of works are currently carried out on that topic, initially for medical and security applications, and more recently for NDT. Available detectors combine a dedicated electronic circuit and a coarse energy resolution obtained with a finite number of counters for each pixel. Associated to MultiX, LETI has developed a new detector capable of taking high-resolution spectrometric measurements, providing spectra with 1keV width bins [5].

The purpose of this study is to present recent developments of Sindbad considering such spectroscopic detectors. These ones have been modelled and integrated into Sindbad, offering spectral imaging functionalities in radiography and tomographic mode. Examples of simulated images are presented in the paper, as well as some experimental validation performed with our spectrometric detector. We conclude by a simulation study which demonstrates the influence of detector characteristics upon beam-hardening effect.

2. Spectral Imaging Simulation

2.1 Overview of Sindbad software

The simulation software Sindbad has been developed to model any radiographic system [1]. Its architecture is divided into three parts: photon beam generation in the X-ray source, beam interaction inside the matter and imaging process. Moreover, functionality has been developed on top of Sindbad to mimic CT acquisitions by allowing the simulation of a series of projections, possibly with rotation and translation of the X-ray system (Fig. 1).

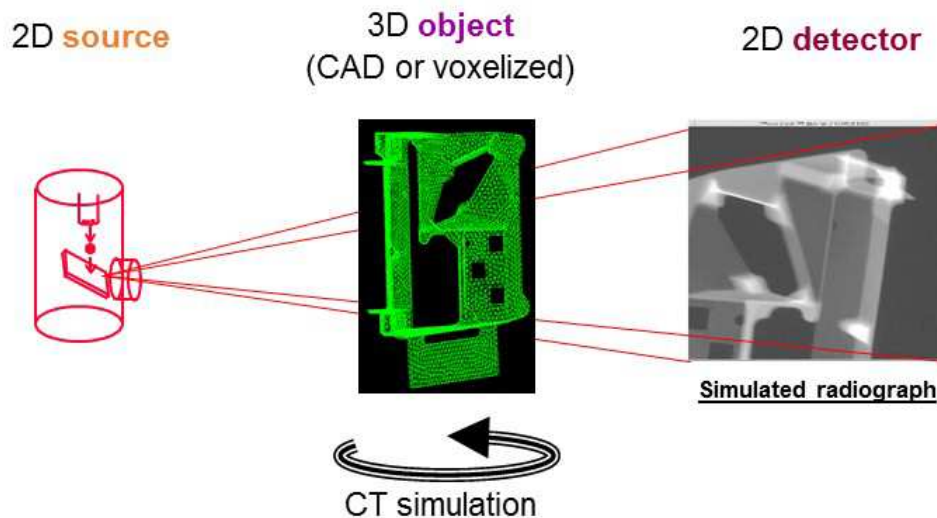


Figure 1. Sindbad architecture: example of a simulation of an industrial part, in radiographic mode. Tomographic (CT) mode is also possible (addition of rotation and /or translation loops).

Concerning the X-ray beam generation in the source, the user can use either an X-ray tube model, for voltage between 30 and 450kV, or any experimental data. Complex industrial parts can be handled by Sindbad, under voxelized or CAD format. Regarding the interaction of particles within the sample, Sindbad performs an analytical and a Monte Carlo simulation respectively for the computation of the primary and of the scatter image. The two approaches can be combined to obtain in a reasonable computing time realistic simulated images including the two components [2].

Finally, Sindbad proposes various detectors models (film, flat panel, scintillating screen coupled to CCD camera, photomultiplier) that differ in the successive physical phenomena involved in the energy to measured signal transform. However, all the considered detectors provide a single value, corresponding to the deposited energy integrated over the energy range (so called integration mode).

Most of the model functionalities of Sindbad has been integrated in the RT simulation module of the CIVA software platform. CIVA software [6], initially developed by CEA-LIST with other partners, is currently distributed (CIVA version 11) by Extende [7]. CIVA deals also with ultrasonic testing and eddy current techniques, and thus offers a simulation package joining together all NDT control techniques. The CIVA package brings together imaging, processing and simulation tools in the same environment, thus enables the interpretation and expertise of simulation and experimental results.

2.2 Modelling the Detector Response Matrix

Semiconductor (CdTe or CZT) based detectors have shown outstanding performance for X-ray or Gamma-ray spectrometry when operating at room temperature. Thanks to a direct conversion from photon to charges that are collected, they are able to count the photons in each energy channel, at high count rates.

As in other previous works [8], [9], an accurate model of a semiconductor detector [10] has been developed in our lab to predict the detector response at any energy. Based on a Monte Carlo code (Penelope [11]), this model first simulates all physical interactions of photons and electrons inside the crystal to provide the position and the number of carriers created at each interaction. Then, a numerical integration of the Shockley-Ramo theorem [12] is performed for each cloud of carriers along their trajectory toward the collecting anodes. Drift transport, diffusion, trapping and charge sharing are taken into account to compute the accurate transient signals induced both on collecting and neighbor anodes. Electronics modelling is finally performed to provide the final pulse waveforms and noise.

The detector response is calculated over all energies and the result stored in a matrix format (Detector Response Matrix, DRM). Fig. 2 presents the matrix of a linear detector 3mm thick, 800 μ m pitch, while Fig. 3 displays the comparison of profiles at 80keV for a linear detector 800 μ m pitch and a matrix detector 500 μ m pitch.

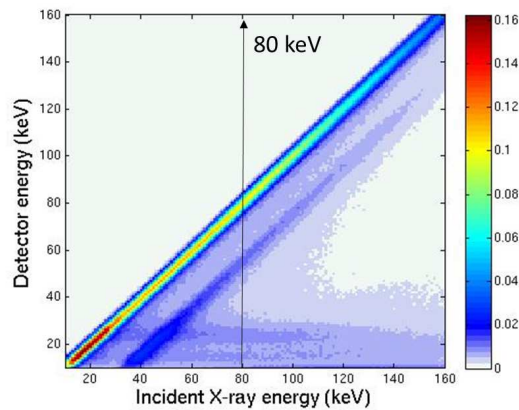


Figure 2. Detector Response Matrix (DRM) for a linear CdTe detector, 800 μ m pitch, 3mm thick, 70ns dead time.

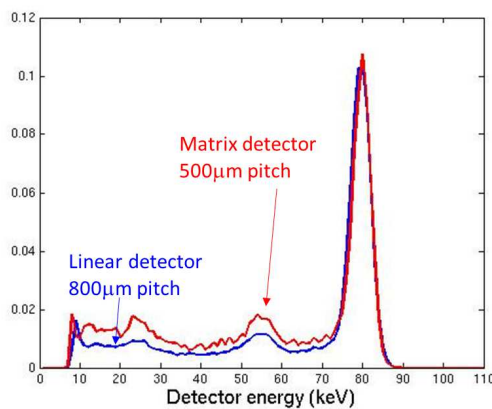


Figure 3. Profile at 80keV of the matrix of Fig. 2 (blue) superimposed to the one with a matrix detector 500 μ m pitch (red). At 80keV the energy resolution is FWHM=5.6keV and charge sharing ratio (counts outside-peak/inside-peak)=0.9. For the 500 μ m pitch detector these values are respectively 5.2 and 1.5.

2.3 Integration of the DRM in Sindbad

This detector model has been integrated into Sindbad to allow providing realistic spectral radiographs of any object. For each pixel, Sindbad first computes the spectrum of photons at the entrance of the detector. This vector is then multiplied by the DRM to obtain the vector representing the measured spectrum.

Fig. 4 shows an example of a spectral imaging simulation in a scanner mode (fan beam geometry). The improbable phantom is a ring made of rubber (Polyisobutene C_4H_8), external diameter 10cm, containing inclusions of nylon ($C_{12}H_{22}N_2O_2$), of foam (PMI, variable densities from 0.8 to 1.1 gcm^{-3}) and of aluminum. After having produced a set of radiographs acquired in tomographic geometry, a standard reconstruction algorithm has been applied for each energy channel. Preliminary to the reconstruction, a grouping of the elementary channels into larger ones was performed. Fig. 4 displays some reconstructed CT slices for two counters. The zooms on right show an insert of nylon, which is brighter than the background in both images, and an insert of foam (0.8 gcm^{-3}) which is brighter in low energy image and darker in high energy image, which confirms the energy dependency of spectral image contrast.

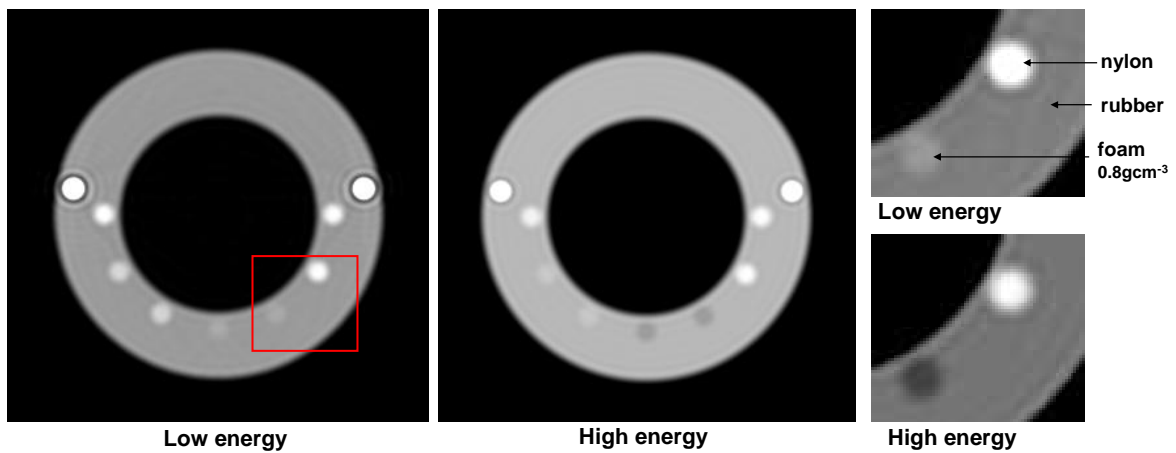


Figure 4. Example of a spectral CT simulation with a CdTe detector. CT slices for two counters (left: 10-25keV; right: 30-80keV). On right, zoom on two inserts (nylon, foam).

2.4 Modelling pileup effect

Pile-up events occur when the interval of two photons interacting into the detector is smaller than the time required for processing one photon (typically 70ns), thus pile-up is particularly important at high photon fluxes. Pile-up results in loss of count-rate and distortion of the energy spectrum. Various models have been proposed in order to compute the detector count statistics. We developed an analytical formalism closed to [13] describing a first order pile-up model of a non-paralyzable detector, with triangular pulse shape. We assume a second order model, corresponding to the possible interaction of two photons only.

Pile-up effect is not linear and the pile-up model cannot be integrated into the DRM. The corresponding transform has to be applied on each pixel of the spectral radiograph provided by Sindbad.

3. Experimental validation

3.1 Validation of a quasi-monochromatic spectrum

Spectra have been acquired using a home-developed 16 pixel linear array CdTe detector. The CdTe crystal is 3mm thick and the pixel pitch is 0.8mm. The detector is coupled to a fast read-out electronic circuit that provides fully resolved energy spectra over 256 bins for each pixel [5]. Spectra have then been corrected for energy-axis scaling using a main-peak edge-driven algorithm. A linear amplitude correction has also been performed by normalizing the total photon count between 66 and 120keV.

The tungsten-target x-ray source has been modelled with an anode voltage of 120kV and a current flow of 10mA. In order to obtain a quasi-monochromatic beam, 2.5mm of lead have been used to filter the x-ray beam, leading to a detector-incident spectrum of about 5keV full width at half height (FWHM).

A spectrum have been simulated by using the Detector Response Matrix (DRM) generated by the detector model (see section 2.2) with geometric and electronic parameters corresponding to the real detector. In order to model additional electronic noise, the detector response has been further convolved with a Gaussian spectrum. The parameter of the Gaussian curve (FWHM of 3.7keV) has been roughly optimized to match that of the acquired data. Photon pile-up, as well as diffusion has not been taken into account, as experimental conditions have been optimized in order to minimize these effects.

Fig. 5 shows the good match between the expected and the acquired spectra, especially at energies higher than 30keV. Furthermore, the influence of the DRM can be clearly observed when comparing the simulated detector-incident spectrum (black) with the measured spectra.

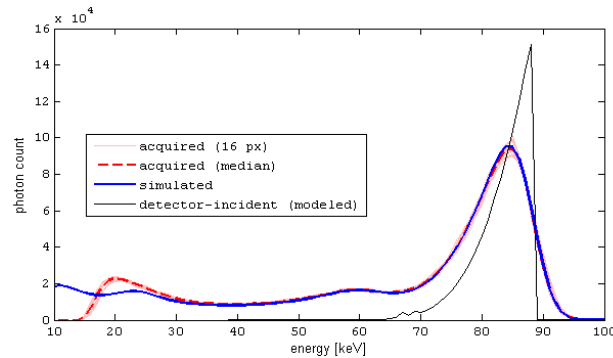


Figure 5. Comparison of acquired (light red) and simulated (blue) spectra generated using a quasi-monochromatic source setup. The median (dotted red) of the 16 acquired spectra is shown for better comparison. The fine black line shows the detector-incident quasi-monochromatic spectrum, corresponding to a 120kV & 10mA Tungsten-anode x-ray generator subsequently filtered by 2.5mm of lead.

3.2 Validation of attenuation measurements

In order to illustrate the benefits of spectral counter detectors compared to energy-integrating detectors, the object in Fig. 6a has been imaged using the same detector as in section 3.1. The object is a cube of 60mm of PE, with three inserts consisting of 42mm POM, 34mm PVDF and 21mm PVC. The source is similar to the one described in section 3.1 but the current flow is limited to 0.2mA and the filtering consists solely of 2mm of Aluminum. The PE cube was placed on a test bench with two moving axes to provide a full field image of the object.

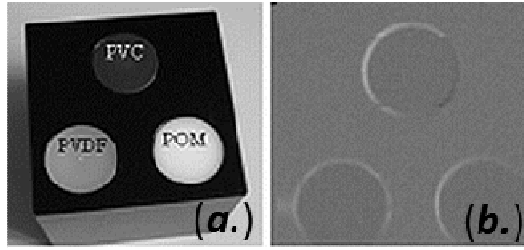


Figure 6. PVC (thickness = 22mm) PVDF (34mm) and POM (42mm) cylinders lodged in a 60x60x60mm³ polyethylene cube (a). In the total attenuation image (b) the different material zone can hardly be distinguished.

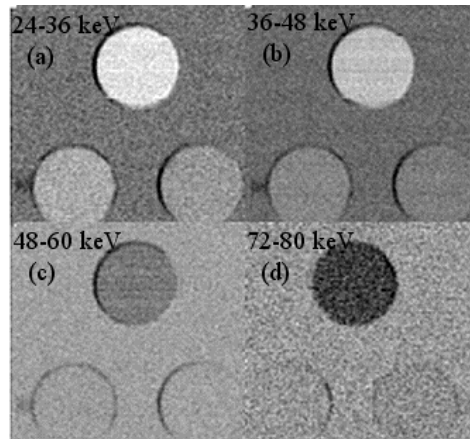


Figure 7. Four energy bin radiograph of the object represented in Figure 6, obtained simultaneously in one acquisition with the CdTe detector and 120kV-0.5mA X-ray source.

The total attenuation image is obtained by summing the counts of the entire spectrum for each pixel (Fig. 6b). A gain correction was used to account for differences in sensitivity of the pixels. The 3 cylinders have different thicknesses and also linear attenuation coefficients. As a result they have the same total absorption and can hardly be distinguished from the polyethylene cube. However, in the case of thinner energy bins, the difference between the materials becomes clear (Fig. 7).

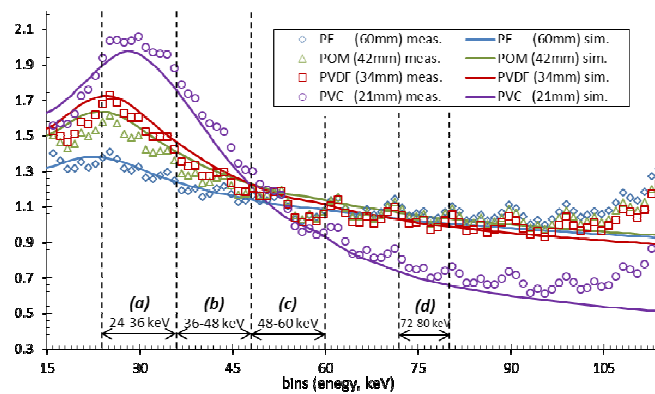


Figure 8. Measured (markers) versus simulated (solid lines) attenuations functions for 60 mm PE, 42mm POM, 34mm PVDF and 21mm PVC.

The contrast differences observed in different energy regions can be explained by the attenuation functions of the irradiated materials. To further understand the difference, the same acquisition has been simulated using the detector model presented in section 2.2.

Fig. 8 shows the comparison between the simulated attenuation (full lines) and the mean measured attenuation (markers). The simulation fits the measures, with the exception of two phenomena: (1) the difference for high energy bins (>100keV), mainly due to photon pile-up, and (2) a pixel-specific oscillation that affect all the four attenuation measurements. This last effect is a measurement artefact (due to the convertor), but it does not call into question the accuracy of the simulation result.

4. Quantification of beam hardening effect and its spectral dependency

The developed simulation tool is useful for the analysis of various CT artefacts induced by the non-linearities of the measurement process, and helps the design of multi-spectral processing correction methods. In this paragraph we present an evaluation of the so-called cupping artefact visible on reconstructed images, due to the beam-hardening of the incident photon flux when crossing the object. In fact this effect is due to the combination of two aspects: the energy dependency of the absorption function, and the non-linearities of the measurement process which depends on detector characteristics. Spectral Sindbad tool allows to quantify the influence of the detector characteristics and bins configuration on this artefact.

By simulation we compute the attenuation measurement value, length-normalized, through an homogeneous material. More precisely we compute:

$$att_{norm} = \frac{1}{l} \log\left(\frac{I_0}{I}\right)$$

where I (resp. I_0) is the measured signal with (resp. without) the object, and l the length of the considered sample.

Of course for a perfect detector and monochromatic flux, the result is independent on l :

$$att_{norm}(E) = \frac{1}{l} \log(e^{\mu(E)l}) = \mu(E)$$

Fig. 9 presents the case of RTM6 resin ($C_{12}O_6H_{22}$). Using an ideal spectral detector (DRM= Identity matrix), 1 keV width channels, we are in the condition of the above equation, and the obtained att_{norm} value is very close to the theoretical one (drawn in black). In the figure $att_{norm}(E)$ is also given for a realistic detector (500 μ m pitch, DRM illustrated in Fig. 2), for various length values l (1mm, 5, 10, 20cm). The obtained functions $att_{norm}(E)$ are clearly dependant on l , especially at low energy.

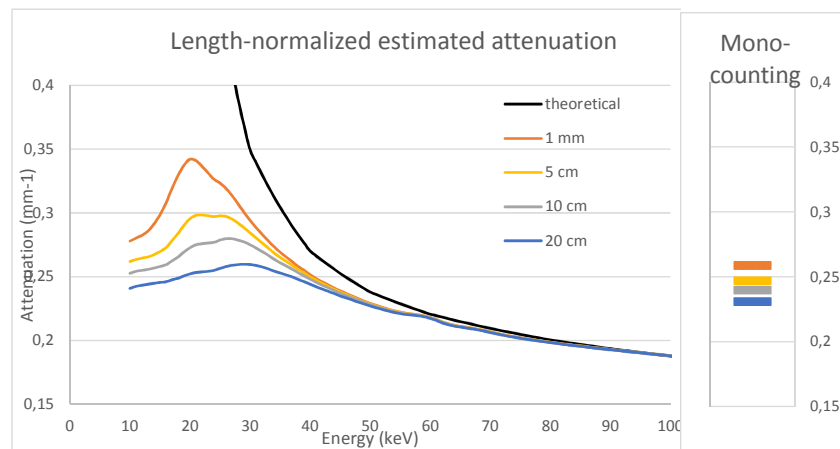


Figure 9. Length-normalized measured attenuation, for various length values (DRM 500 μ m). Resin material. On right: mono-counting configuration.

On Fig.9-right, the single value obtained in mono-counting mode (summing all contribution of energy channels) is represented. Also the length-dependency is visible, this is the well-known beam-hardening artefact. Fig9-left illustrates the spectral behavior of that effect.

Images of a homogeneous cylinder of the same material (RTM6), 300mm diameter, are reconstructed from simulated projections, obtained without noise (Fig. 10). Two detectors are considered, the ideal and the realistic ones used previously. Images are reconstructed for each 1keV bin, which is possible thanks to the lack of noise. The ideal one is also considered in the mono-counting configuration (summation of the number of photons on the whole energy range 10-120keV).

On Fig. 10 the well-known cupping artefact is clearly visible (image, and blue profile) for the mono-counting configuration, due to the large energy range. Profiles are also drawn for the 40keV bin when using the ideal detector (black profile) and the spectral one (red profile). The artefact is almost no more observable for the ideal detector, but is present for the realistic one. The fact to dispose of 1keV width bins makes the system linear in case of an ideal detector – in fact the linear Beer-Lambert law relying attenuation and thickness is valid, but when using realistic detectors, the system is no longer linear even for 1keV width bins. Charge sharing phenomenon that induces tailing in the detector response spectra has particularly strong influence on non-linearities.

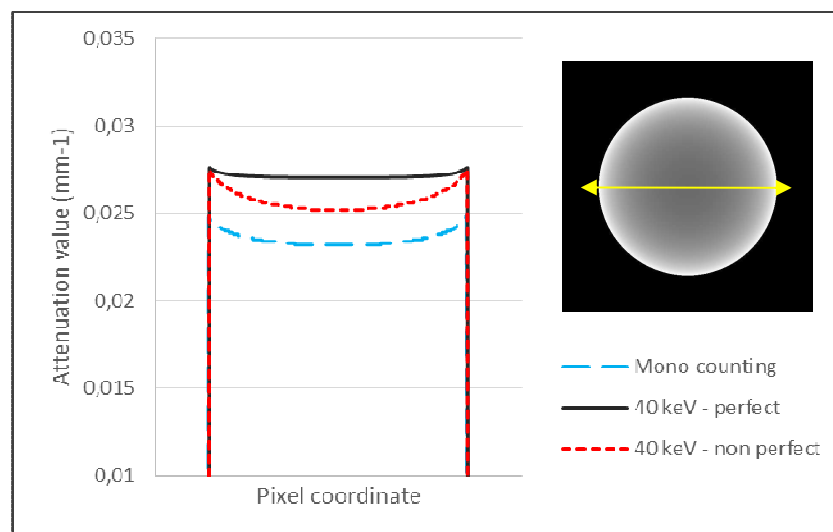


Figure 10. Profiles on a reconstructed RTM6 cylinder, for various detector configurations. Image for mono-counting configuration.

5. Conclusion

We have developed new functionalities of Sindbad software for spectral X-ray imaging simulation. A detector response matrix is computed, then coupled to the ray-tracing and radiograph simulation module. Experimental validation of the model has been performed, using for comparison a semi-conductor detector developed in our laboratory. This new version of Sindbad allows the analysis of the influence of detector characteristics (geometry, material, electronics...) and detector configuration (number and boundaries of channels) on image quality. The final objective is to help dedicated detector design and optimization. It is also an essential tool for the development and validation of multi-spectral processing methods. Current developments concern the simulation of the scatter radiation in spectral

mode [14]. Future developments will address more complex models of pile-up effect for high photon fluxes.

References

1. J. Tabary, P. Hugonnard & F. Mathy, "SINDBAD : a realistic multi-purpose and scalable X-ray simulation tool for NDT applications," Int. Symp. on DIR and CT, Lyon, June 2007.
2. J. Tabary, A. Glière, R. Guillemaud, P. Hugonnard, F. Mathy, 'Combination of high resolution analytically computed uncollided flux images with low resolution Monte Carlo computed scattered flux images', IEEE TNS, Vol. 51, No. 1, pp 212-217, February 2004.
3. J. S. Iwaczyk, E. Nygard, O. Meirav, J. Arenson, W.C. Barber, N.E. Hartsough, N. Malakhov & J.C. Wessel, "Photon counting Energy Dispersive Detector Arrays for X-ray Imaging," IEEE TNS, Vol. 56 (3), pp. 535-542, 2009.
4. C. Szeles, S. A. Soldner, S. Vydrin, J. Graves, & D.S. Bale, "CdZnTe Semiconductor Detectors for Spectrometric X-ray Imaging," IEEE TNS Vol. 55 (1), pp. 572-582, 2008.
5. A. Brambilla, P. Ouvrier-Buffet, J. Rinkel, G. Gonon, C. Boudou & L. Verger, "CdTe linear pixel X-ray detector with enhanced spectrometric performance for high flux X-ray imaging," IEEE TNS, vol 59, pp 1552-1558, 2012.
6. P. Calmon, S. Mahaut, S. Chatillon and R. Raillon, 'CIVA: An expertise platform for simulation and processing NDT data', Proc. of Ultrasonics International (UI'05) and World Congress on Ultrasonics (WCU), vol. 44, sup. 1, pp 975-979, December 2006. Available: <http://www-civa.cea.fr>.
7. Available: <http://www.extende.com/>
8. E. Roessl, H. Daerr, K. J. Engel, A. Thran, C. Schirra & R. Proksa, "Combined effects of pulse pile-up and energy response in energy-resolved, photon-counting computed tomography," IEEE Nucl. Sci. Symp. Conf. record 2011.
9. M. Benoit & L. A. Hamel, "Simulation of charge collection processes in semiconductor CdZnTe γ -ray detectors", NIM A, vol 606, pp 508-516, 2009.
10. G. Montémont, M-C. Gentet, O. Monnet, J. Rustique & L. Verger, "Simulation and Design of Orthogonal Capacitive Strip CdZnTe Detectors", IEEE TNS, vol. 54, issue 4, pp. 854-859, 2007
11. J. Sempau, E. Acosta, J. Baro, J.M. Fernandez-Varea and F.Salvat, "An algorithm for Monte Carlo simulation of the coupled electron-photon transport", NIM B 132, pp.377-390, 1997.
12. S. Ramo, "Currents Induced by Electron Motion," Proc. I.R.E. vol. 27, pp.584-585, 1939.
13. K. Taguchi, E.C. Frey, X. Wang, J.S. Iwaczyk, et W.C. Barber. « An Analytical Model of the Effects of Pulse Pileup on the Energy Spectrum Recorded by Energy Resolved Photon Counting X-Ray Detectors ». In Progress in Biomedical Optics and Imaging - Proceedings of SPIE. Vol. 7622, 2010. doi:10.1117/12.843753.
14. A. Sossin, J. Tabary, V. Rebuffel, JM. Letang, N. Freud, L. Verger, "Fast Scattering Simulation Tool for Multi-Energy X-ray Imaging", Proc. IEEE-MIC, November 2014.